

Morphological Identification of Wide-Separation Gravitationally Lensed Quasars

Pranav Sivakumar¹

ABSTRACT

A novel method was developed to identify gravitationally lensed quasars from the Sloan Digital Sky Survey (SDSS). Understanding gravitational lensing can help decipher the properties of dark matter and dark energy. It is hypothesized that if multiple objects in an SDSS image meet both photometric and spectral criteria, then these objects are gravitationally lensed quasar candidates. The first phase of this project used data from the SDSS Data Release 9. In the follow-up study, the method was improved upon and extended using the SDSS Data Release 10, which included data for over 300,000 quasars. The SDSS data was retrieved and processed using Structured Query Language (SQL) queries. Using this information, the algorithm compared the quasars to their neighbors to determine if the neighbors were images of the same quasar. The results were validated against a control group of lensed quasars reported in the literature. Statistical analyses were also performed to ensure that the comparison parameters were consistent across the data set. A comparison of the project's results with established data sets of lensed quasars led to the conclusion that the hypothesis was well supported. In addition to identifying a majority of the quasars in the control group, the algorithm also identified additional high-probability lens candidates not reported in the literature.

¹ Barrington High School, 616 West Main Street, Barrington, IL 60010

Introduction

The purpose of this project is to develop a novel technique for identifying gravitationally lensed quasar candidates. Quasars, also known as QSOs (quasi-stellar objects), are point-like luminous astronomical objects located around supermassive galactic black holes. QSOs are some of the oldest and farthest objects known. Since they are very distant, the electromagnetic radiation coming from them can be affected by the masses of their host galaxies, as well as other objects between Earth and the quasars.

General relativity predicted that the gravitational pull of a massive object can distort the light of an object far away. This phenomenon, known as gravitational lensing, can make an object appear much brighter and produces multiple images of the object. Gravitational lensing, popularly known as "Cosmic Mirage", was first observed in quasars in 1979. Since that discovery, over 100 gravitationally lensed quasars have been confirmed.

Gravitational lensing can be used to explore cosmology and the structures of astronomical objects. It can help scientists learn about the properties of dark matter and dark energy and can validate cosmological parameters such as the Hubble constant. It is the only method that probes distributions of dark matter directly, since lensing is a purely gravitational phenomenon.

Lensed quasars can be identified from observations in the optical, radio and other bands of the electromagnetic spectrum. Each of these methods has unique advantages and disadvantages. This research project used observations in bands ranging from ultraviolet to far infrared.

The observational data is compiled from one of the most comprehensive sky surveys – the Sloan Digital Sky Survey (SDSS). The SDSS is a photometric and spectroscopic survey of one-fourth

of the Northern Hemisphere sky. The surveys were carried out using a wide-field 2.5-meter telescope at the Apache Point Observatory in New Mexico.

The first iteration of the research project, detailed in Sivakumar (2013), used the SDSS Data Release 9 (DR9). This follow-up research addresses some of the limitations and shortcomings of the previous work and also incorporates an extended data set from the SDSS Data Release 10 (DR10), described in Ahn et al. (2013).

In addition, this project used results from the FIRST (Faint Images of the Radio Sky at Twenty-Centimeters), ROSAT (ROentgen SATellite), and WISE (Wide-field Infrared Survey Explorer) surveys for additional confirmation of candidate lensed quasars. Each of these surveys had objects that corresponded to SDSS objects. Wherever the cross-references existed, they were used to check for objects with comparable characteristics in other bands.

The following hypothesis is proposed for this research project:

“If multiple objects in an SDSS image meet both photometric and spectral criteria, then these objects are high-probability gravitationally lensed quasar candidates because they are virtual images of the same quasar.”

Review of Literature

Due to its importance and the availability of large data sets, quasar lensing is an active area of research and a number of papers on the subject have been published over the last 25 years.

Turner, Ostriker, and Gott (1984) first explored quasar lensing probabilities due to galaxies and the resulting image separation distributions. This work laid the foundation for the study of quasar lensing. Since this original research, many scientists have developed efficient and reliable ways to identify lensed quasars.

Most of the methods fall into one of two categories; those based on photometric and spectral characteristics of quasars observed in the optical wavelengths, and those that use radio data. Statistical samples of strongly lensed quasars have been constructed at both radio and optical wavelengths.

The Hubble Space Telescope (HST) Snapshot Survey was the first large lensed quasar survey, covering a set of 498 quasars from established astronomical catalogs. The analysis of the survey results by Maoz et al. (1993) showed that about 1% of luminous quasars at $z > 1$ (z = redshift) are gravitationally lensed into multiple images with separations in a 0.1 to 7 arcsecond range.

Oguri et al. (2006) presented an algorithm to identify gravitationally lensed quasar candidates which eventually led to the creation of the SDSS Quasar Lens Search (SQLS). The algorithm used photometric and color selection criteria to identify small- and large-separation lenses, respectively. A statistically valid set of 11 lensed quasars was created by Inada et al. (2008) based on the SQLS catalog. Of these, 10 were galaxy-scale lenses with small image separations ($\sim 1''\text{--}2''$) and one was a large separation (15'') system produced by a massive galaxy cluster.

Oguri et al. (2012) report the results of applying the statistical sampling of lensed quasars to study the limits on the value of the cosmological constant and dark energy distribution. By comparing the observed lensing probability with theoretical predictions, Oguri's results support the accelerated cosmic expansion theory.

Since quasars were first detected through radio telescopes, there exists a large body of research related to quasar lensing using radio astronomy. The Cosmic-Lens All Sky Survey (CLASS), by Browne et al. (2003), discovered 22 gravitational lenses from about 16,000 radio sources.

The FIRST radio survey covered the same part of the sky as the SDSS. Schechter, Gregg, Becker, Helfand, and White (1998) reported the first lensed quasar identified by the FIRST survey (FBQ 0951+26351.1) by comparing the separation, magnitude and radio signatures of its two images.

Prior to this project, quasar lensing research in optical bands focused solely on either photometric or spectral characteristics of quasars. The candidate selection algorithm developed in this research project combines both types of data to identify potential lensing candidates.

Methods of Procedure

This research project uses a morphological approach for finding candidate lists of lensed quasars in the SDSS DR10. The candidate list from this project is validated against the Master Lens Database, described in Moustakas et al. (2012). The Master Lens Database is a compilation of lensed quasars reported in the literature and includes 120 lensed quasars from SQLS, CLASS, HST, and other smaller surveys.

In order to create a statistically representative set of lensed quasar candidates, it is important to begin with a large sample of quasars. The SDSS Data Release 10 provides a robust and uniform selection of over 300,000 quasars with high-quality photometric and spectral data.

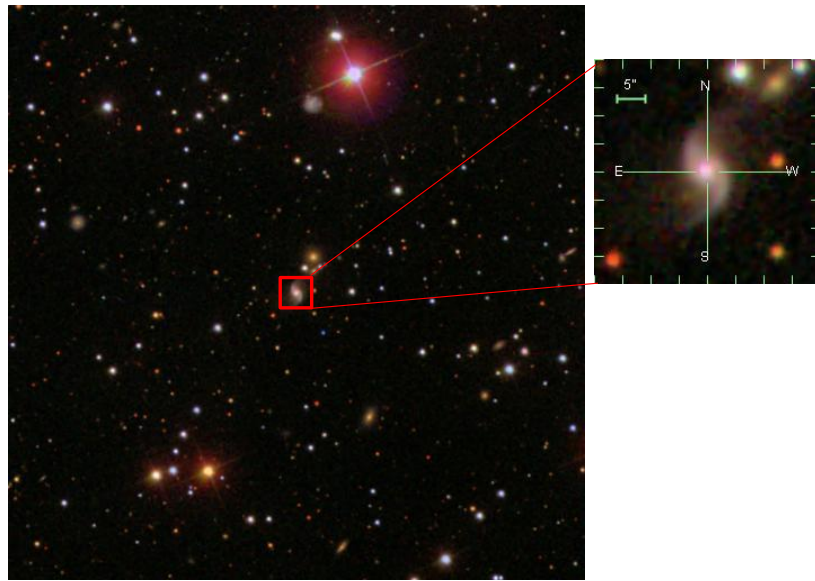


Figure 1: SDSS Image of a Typical Quasar (SDSS J205141.54+005135.4)

A representative SDSS image of a quasar is shown in Figure 1. This particular quasar is seen inside its background galaxy. Quasars are so far away that most look like single bright points in the sky -- just like normal stars. When the PHOTO pipeline of the SDSS processes an image, it does not have enough information to differentiate between a star and a quasar because they are

both point sources. In order to distinguish between the two, the SDSS pipeline uses non-photometric data such as an object's colors or its spectrum. While the spectra of stars are roughly blackbody in shape, those of quasars are characterized by strong emission lines. In addition, quasars are so distant that their spectra are highly redshifted. In order to find quasars from a set of candidates, the SDSS pipeline searches for the presence of strong emission lines in spectra.

The hydrogen-alpha line of the spectrum in Figure 2 lies in the range of 7,100 to 7,400 angstroms with a peak at around 7,300 angstroms. This emission line is indicative of a quasar.

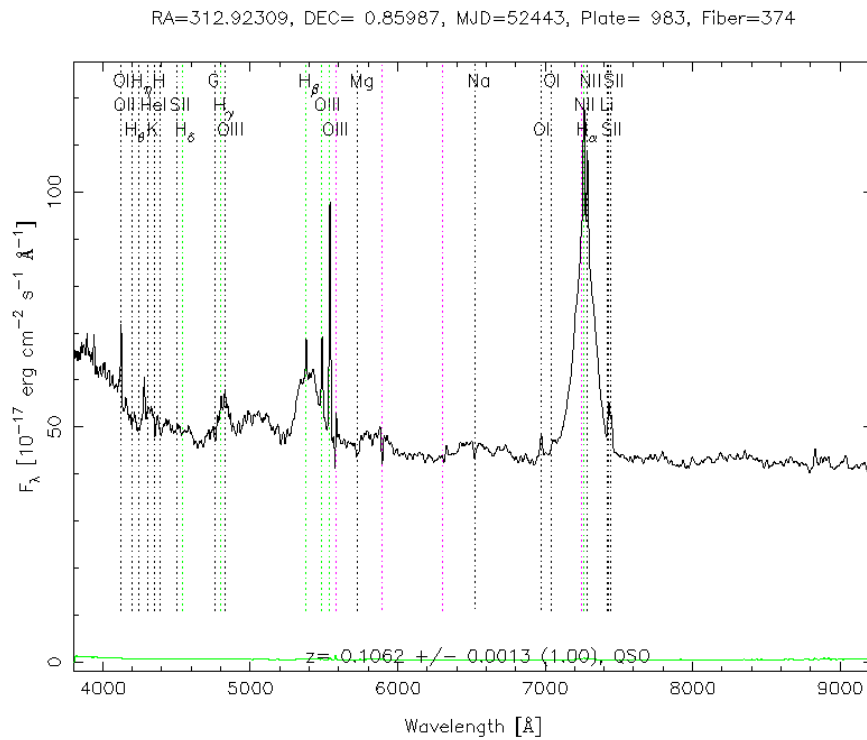


Figure 2: The SDSS spectrum of a typical quasar (SDSS J205141.54+005135.4) from the SDSS DR10 data set. Each of the peaks in the graph represents an emission line, while each valley represents an absorption line.

The rest frame hydrogen-alpha emission line has a rest-frame wavelength of 6,565 angstroms. In quasar spectra, the hydrogen-alpha line is usually at a longer wavelength. The difference between the measured emission line peak and the rest-frame value is used to compute the

redshift of the object. The "z" value at the bottom of the image shows the redshift. Using the redshift of an astronomical object, the time at which light left the object and its distance from Earth can be calculated using standard cosmological models. The most distant quasar identified by the SDSS has a redshift of around 7.2; according to the cosmological calculator from Wright (2006), it existed around 700 million years after the Big Bang. The farthest known astronomical object, UDFj-39546284, has a redshift of 11.9.

While the quasar redshifts plotted in Figure 3 range from 0 to 7, most redshifts lie between 1 and 3. One can discern from these redshift values that quasars existed during very early periods of the Universe.

Measured redshift	Age at redshift (giga light years)	Light travel time (giga light years)
1	5.935	7.731
2	3.342	10.324
3	2.190	11.476
4	1.571	12.094
5	1.197	12.469
6	0.950	12.715
7	0.778	12.888
8	0.651	13.014
11.9	0.379	13.286

Table 1: Calculated Values of Age and Distance for Different Redshifts

The SDSS measures magnitudes of astronomical objects in five different wavelengths by capturing images through ultraviolet (u), green (g), red (r), and two infrared (i and z) color filters. The measured magnitude through any filter does not represent an object's real color. For this reason, color differences are used to compare target quasar and potential lens candidates.

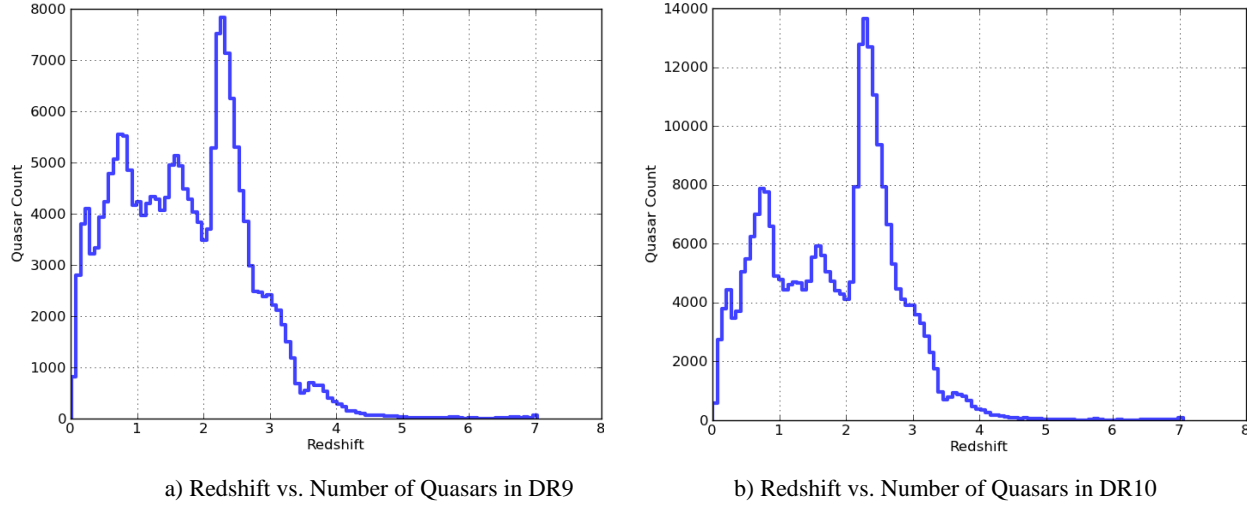


Figure 3: Histograms of SDSS quasar redshifts. The histograms show the number of quasars in the DR9 and DR10 data sets for each redshift range. The histograms are very similar; the only noticeable differences are the proportionately larger number of DR10 quasars at $z \approx 0.8$ and $z \approx 2.3$.

Throughout this research project, color differences are used to compare target quasar and potential lens candidates. Specifically, $u-g$, $g-r$, and $r-i$ colors are used. In the SDSS data set, z magnitudes have higher error margins and are not used in this study. Figure 4 is a plot of $g-r$ values for all the quasars in the SDSS DR10. The concentration of most of the data points below a $g-r$ value of 1 indicates that a majority of the quasars have similar color characteristics.

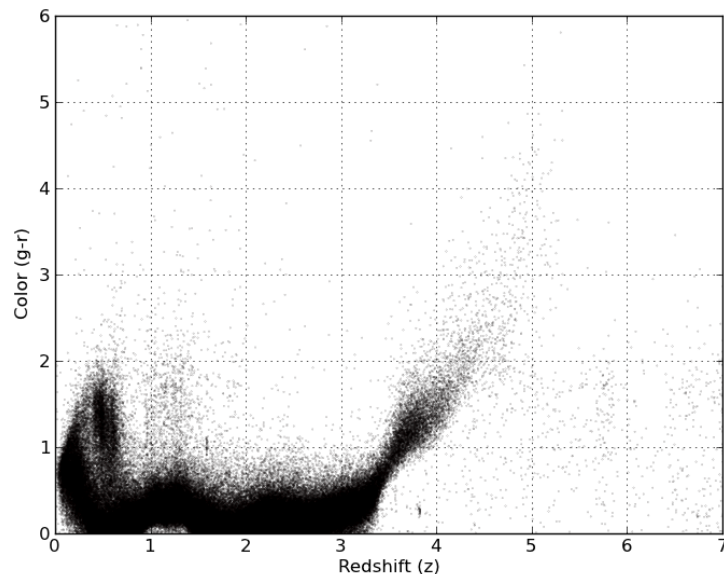


Figure 4: Color Graph of Quasar Population

Candidate Identification Algorithm

The algorithm used in this project was originally proposed in Sivakumar (2013). This project followed up on that earlier paper and made several improvements; it improved on the selection methods of the previous algorithm, expanded the data set by including 100,000 more quasars from the SDSS DR10, validated results against a more comprehensive control group and incorporated additional validation criteria from infrared and X-ray sky surveys.

The candidate selection algorithm begins with a list of all objects classified as QSOs by the SDSS pipeline. The pipeline uses a detailed set of steps to identify these QSOs, but it sometimes misses objects spread over a large area. In order to fill this gap, a query using the unique color characteristics of quasars was developed. This query utilized the guidelines for color cuts from Richards et al. (2001). The two data sets were combined and duplicates were removed, resulting in a baseline data set of 532,704 quasar candidates. This data set is significantly larger than the data set for DR9 collected using the same method. The data set used in this project is also more comprehensive, as it incorporates over 3 times the number of candidate quasars considered in Oguri et al (2012).

One of the shortcomings of the earlier algorithm used in Sivakumar (2013) was that the quasar candidate list only included objects that SDSS identified as sciencePrimary. This limitation eliminated some of the potential lens candidates from consideration. In order to accommodate objects that were not specifically tagged by the SDSS, the spectral data was taken from the SpecPhotoAll table instead of the SpecPhoto view. The SpecPhotoAll table includes photometric parameters of the objects and all of the spectra associated with the objects.

Figure 5 is a location-based plot of all 300,000+ quasars included in the SDSS DR10 data set. Since the SDSS surveys only about one-fourth of the Northern Hemisphere sky, most of the objects are above the galactic equator.

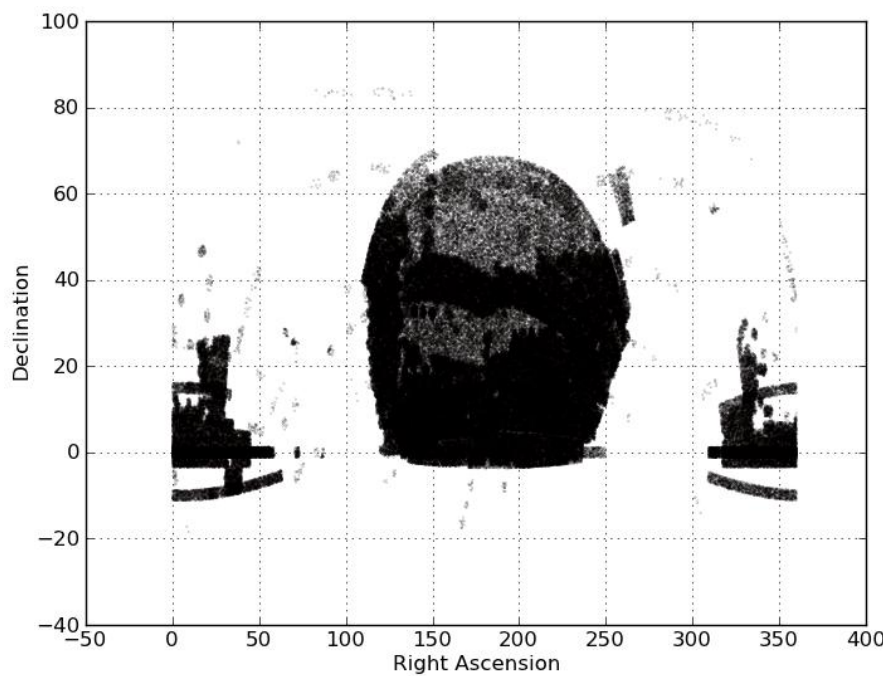


Figure 5: Distribution of Quasars in the Celestial Sphere within SDSS Sky Coverage

The right ascension, which is similar to longitude on the Earth, is plotted on the X-axis, while declination, which is similar to latitude, is plotted on the Y-axis.

The overall candidate selection algorithm is outlined in Figure 6. For each quasar in the baseline data set, all the neighbors within a separation threshold were identified. Separation between objects is defined in terms of angular distance along right ascension and declination. It is typically expressed in terms of arcseconds or arcminutes. Based on analysis of published research literature, a separation value of $16''$ was selected.

The SDSS data set did not have spectral data for all of the neighbors of the target quasars. If the neighbor's spectral data was available, the algorithm compared the redshifts of the neighbor and

the reference quasar; it rejected neighbors with a redshift difference of greater than 0.1. In Sivakumar (2013), the redshift difference criterion was set at 0.01. The new criterion allowed for some error in redshift measurements while ensuring that astronomical objects in the same part of the sky as the quasar but at a different distance were removed from the candidate list.

The $g-r$ color difference of each valid neighboring object was compared with the color of the reference quasar. If a neighboring object had a similar redshift and color composition, there was a high probability that the two images corresponded to the same lensed quasar. If the neighbor did not have spectral data, only the color comparison was performed, and those neighbors that met the criterion were added to one of the low-probability candidate lists.

The color comparison was performed using the functions below:

$$D(i - j) = (i - j)_{\text{quasar}} - (i - j)_{\text{neighbor}}$$

OR

$$D(i - j) = (i - j)_{\text{neighbor}} - (i - j)_{\text{quasar}}$$

where $D(i-j)$ is the color difference between the quasar and its companion in a particular pair of color bands ($(i, j) = (u, g), (g, r), (r, i), (i, z)$).

The algorithm classified the target quasars that matched at least one of the spectral or color criteria into three types. The final outputs from the algorithm were two lists of candidate quasars, a high probability list and a low probability list. The high probability list, which consisted of the first of the three types, contained candidates which matched both the spectral and color criteria. The candidates from this list are ideal targets for further validation. The candidate quasars in the low probability list should be analyzed further in order to qualify as candidates for targeted observation.

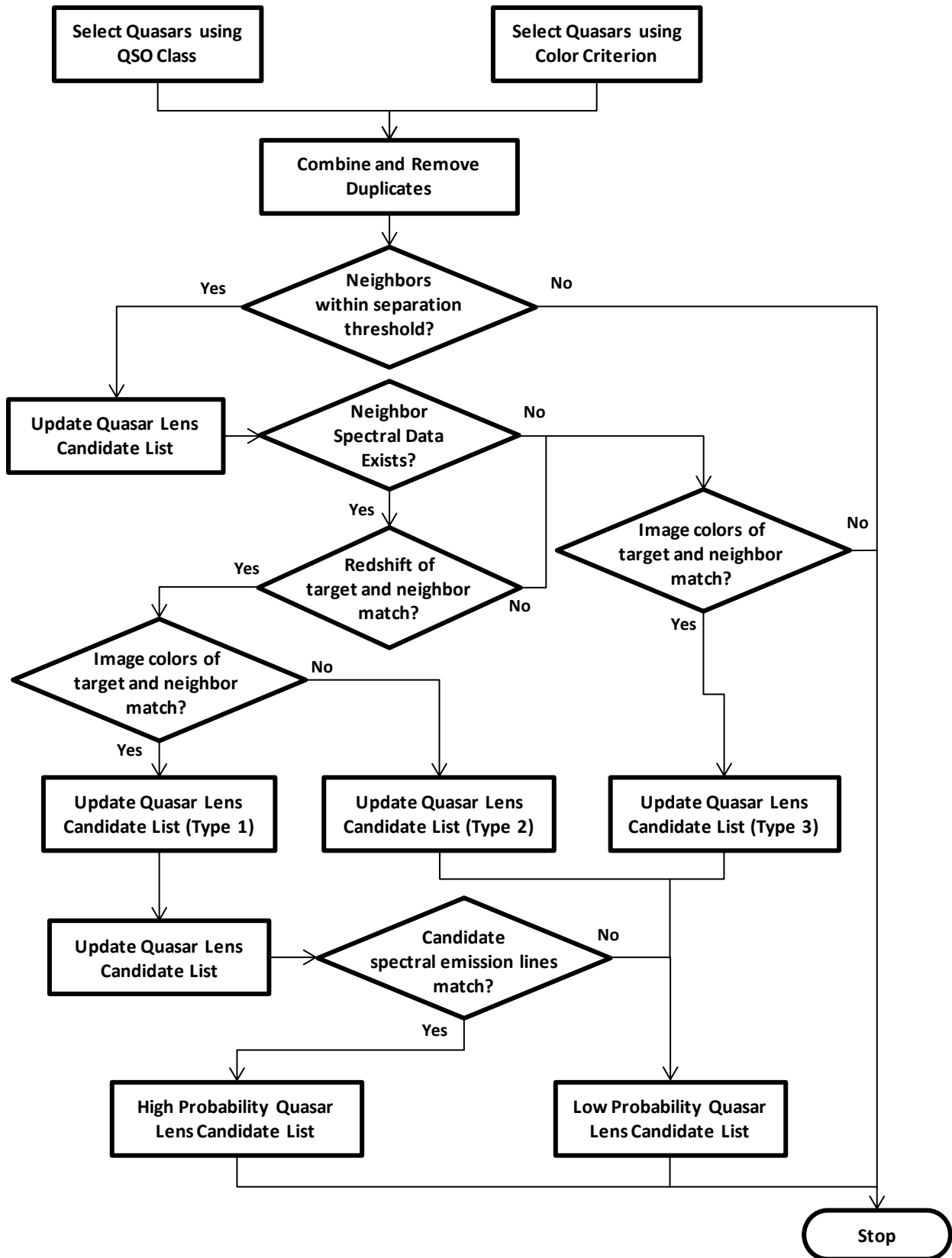


Figure 6: Flowchart of the candidate selection algorithm

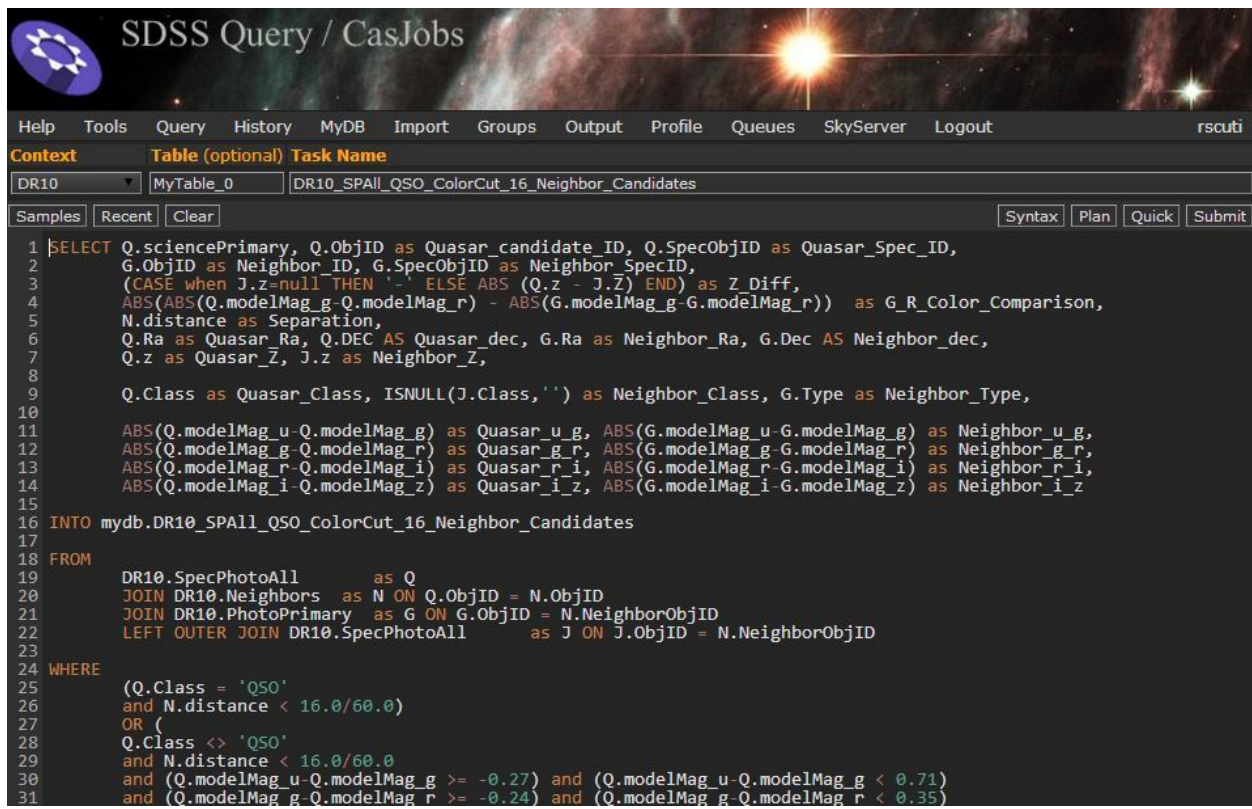
As a final validation step, the spectra of the 279 high-probability candidates were compared against their neighbors' spectra. If the redshifts of two quasars match, the location of their emission lines should also match. The confidence level of the lens candidate was increased if the two spectra were similar.

In order to confirm the quasars at multiple wavelengths, data was taken from the FIRST, ROSAT, and WISE surveys. The FIRST table from the SDSS contained all SDSS objects that had FIRST matches. However, the likelihood of finding a FIRST match for most quasars is not high, as a majority of quasars are radio-quiet. When FIRST matches do exist, they provide a higher degree of confidence; however, non-matches do not rule out the possibility of quasars being lensed. The ROSAT and WISE tables from the SDSS were also utilized in order to find SDSS matches in those data sets; just as in the case of FIRST matches, ROSAT and WISE matches increase the confidence of candidates but do not disprove the presence of lensed quasars.

Results

Data Extraction and Processing

The first steps of data analysis in this project were data extraction and synthesis, criterion matching, and data validation. Structured Query Language (SQL) was used extensively to target, filter and manipulate the DR9 and DR10 data. In order to select the baseline set of quasars, an SQL query was used. This query returned the spectral and photometric parameters needed for different comparison steps in the algorithm. A screenshot of the query is shown in Figure 7.



The screenshot shows the SDSS Query / CasJobs interface. The top navigation bar includes Help, Tools, Query, History, MyDB, Import, Groups, Output, Profile, Queues, SkyServer, and Logout. The user is logged in as 'rscuti'. The main window displays an astronomical image of a galaxy cluster with several bright stars. Below the image is a search bar with 'Context' dropdown set to 'DR10', 'Table (optional)' set to 'MyTable_0', and 'Task Name' set to 'DR10_SPAll_QSO_ColorCut_16_Neighbor_Candidates'. There are tabs for 'Samples', 'Recent', and 'Clear', and buttons for 'Syntax', 'Plan', 'Quick', and 'Submit'. The SQL code is listed below:

```
1 SELECT Q.sciencePrimary, Q.ObjID AS Quasar_candidate_ID, Q.SpecObjID AS Quasar_Spec_ID,
2 G.ObjID AS Neighbor_ID, G.SpecObjID AS Neighbor_SpecID,
3 (CASE WHEN J.z IS NULL THEN '' ELSE ABS(Q.z - J.z) END) AS Z_Diff,
4 ABS(ABS(Q.modelMag_g - Q.modelMag_r) - ABS(G.modelMag_g - G.modelMag_r)) AS G_R_Color_Comparison,
5 N.distance AS Separation,
6 Q.Ra AS Quasar_Ra, Q.DEC AS Quasar_dec, G.Ra AS Neighbor_Ra, G.Dec AS Neighbor_dec,
7 Q.z AS Quasar_Z, J.z AS Neighbor_Z,
8 Q.Class AS Quasar_Class, ISNULL(J.Class, '') AS Neighbor_Class, G.Type AS Neighbor_Type,
10 ABS(Q.modelMag_u - Q.modelMag_g) AS Quasar_u_g, ABS(G.modelMag_u - G.modelMag_g) AS Neighbor_u_g,
12 ABS(Q.modelMag_g - Q.modelMag_r) AS Quasar_g_r, ABS(G.modelMag_g - G.modelMag_r) AS Neighbor_g_r,
13 ABS(Q.modelMag_r - Q.modelMag_i) AS Quasar_r_i, ABS(G.modelMag_r - G.modelMag_i) AS Neighbor_r_i,
14 ABS(Q.modelMag_i - Q.modelMag_z) AS Quasar_i_z, ABS(G.modelMag_i - G.modelMag_z) AS Neighbor_i_z
15
16 INTO mydb.DR10_SPAll_QSO_ColorCut_16_Neighbor_Candidates
17
18 FROM
19   DR10.SpecPhotoAll AS Q
20   JOIN DR10.Neighbors AS N ON Q.ObjID = N.ObjID
21   JOIN DR10.PhotoPrimary AS G ON G.ObjID = N.NeighborObjID
22   LEFT OUTER JOIN DR10.SpecPhotoAll AS J ON J.ObjID = N.NeighborObjID
23
24 WHERE
25   (Q.Class = 'QSO'
26   AND N.distance < 16.0/60.0)
27   OR (
28     Q.Class NOT IN ('QSO')
29     AND N.distance < 16.0/60.0
30     AND (Q.modelMag_u - Q.modelMag_g) >= -0.27 AND (Q.modelMag_u - Q.modelMag_g) < 0.71
31     AND (Q.modelMag_g - Q.modelMag_r) >= -0.24 AND (Q.modelMag_g - Q.modelMag_r) < 0.35)
```

Figure 7: The SQL query to extract data from the DR10 CasJobs data server. The query extracted data for 592,313 neighbors identified as potential lensing candidates.

In the second step, the neighbors within a 16" separation window of the quasars were extracted and manipulated. The separation between two images of the same lensed quasar depends on the mass of the intervening object(s). If these objects are very massive, such as galaxy clusters, the

separation between lens images will tend to be greater than 8''. The image separation also depends on the redshift and hence the distance of the quasar. At 16'' of separation, 592,313 objects were identified as neighbors. In Figure 8, the distribution of neighbors is plotted along the three galactic dimensions using SciPy libraries. The pattern of the distribution in Figure 8 is consistent with the sky coverage of the SDSS shown in Figure 5 and the redshift histogram of the quasars in Figure 3.

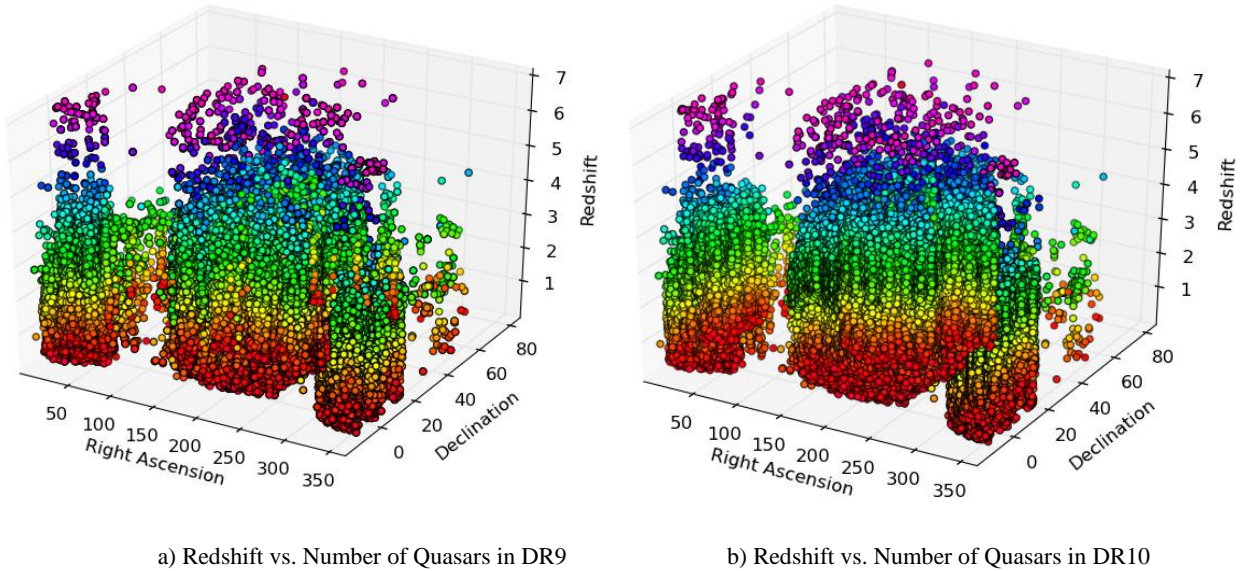


Figure 8: The distribution of neighbors within 16'' of the quasars plotted along the three galactic dimensions.

Figure 9 shows the number of neighbors identified for different values of spatial separation between the target quasar and the neighbor. The counts shown in Figure 9 include only neighbors of target quasars identified as QSOs by the SDSS pipeline.

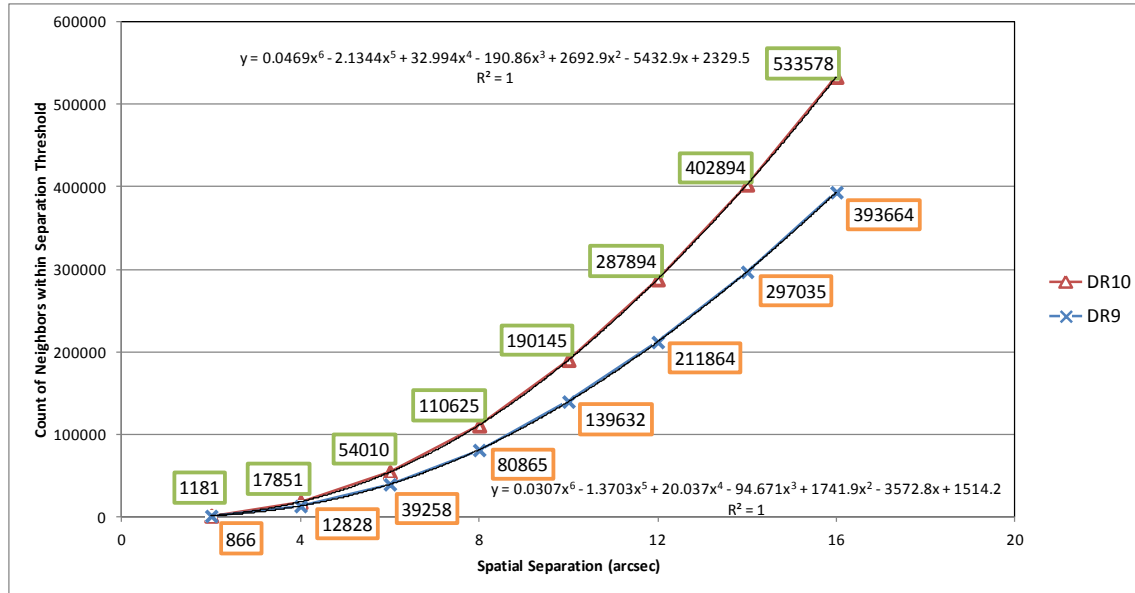


Figure 9: Number of Neighbors vs. Separation

The candidates generated from the morphological algorithm matched the control group of lensed quasars from the literature. Table 2 lists the data coverage, selection criteria, and number of preliminary candidates identified. The use of restrictive redshift and color criteria resulted in a much smaller number of successful matches in Types 1-2 as compared to Type 3.

Candidate List	Scope	Criteria	Number of Candidates
Type 1A	Spectral and Photometric Data	Quasar.Class = 'QSO' and Neighbor.Class = 'QSO' Redshift and Color	55
Type 1B	Spectral and Photometric Data	Quasar.Class = 'QSO' and Neighbor.Class = 'Galaxy' Redshift and Color	111
Type 1C	Spectral and Photometric Data	Quasar.Class = 'Galaxy' and Neighbor.Class = 'QSO' Redshift and Color	0
Type 1D	Spectral and Photometric Data	Quasar.Class = 'Galaxy' and Neighbor.Class = 'Galaxy' Redshift and Color	113
Type 2A	Spectral and Photometric Data	Matched Z-difference and not color criterion Quasar.Class = 'QSO' and Neighbor.Class = 'QSO'	36
Type 2B	Spectral and Photometric Data	Matched Z-difference and not color criterion Quasar.Class = 'QSO' and Neighbor.Class = 'Galaxy'	488
Type 2C	Spectral and Photometric Data	Matched Z-difference and not color criterion Quasar.Class = 'Galaxy' and Neighbor.Class = 'QSO'	2
Type 2D	Spectral and Photometric Data	Matched Z-difference and not color criterion Quasar.Class = 'Galaxy' and Neighbor.Class = 'Galaxy'	352
Type 3	Photometric Data	No Redshift – matched color criterion Color Only	82073

Table 2: Count of candidates for different candidate selection criteria

The Type 1 candidates were further organized into four subtypes based on the SDSS classes of the targets and the neighboring objects. Quasar-quasar lensed candidates were classified as type 1A, quasar-galaxy pairs were labeled as type 1B, galaxy-quasar pairs as type 1C, and galaxy-galaxy pairs as type 1D. The Type 2 candidates were classified according to the same scheme. Since there were no type 1C candidates, the high-probability list consisted of candidates from types 1A, 1B, and 1D. There were Type 2 candidates from all subtypes.

As a final validation step, the spectra of the 279 high probability candidates in Type 1 were compared against their neighbors' spectra. If a neighbor is truly a lensed image of the target quasar, the spectrum of the neighbor should be very similar to the spectrum of the target quasar. Specifically, the location of key emission lines, the width of the emission lines, and the overall shape of the spectra should be comparable.

Candidate List	Scope	Criteria	Number of Candidates
Type 1A	Spectral and Photometric Data	Quasar.Class = ‘QSO’ and Neighbor.Class = ‘QSO’ Redshift and Color	34
Type 1B	Spectral and Photometric Data	Quasar.Class = ‘QSO’ and Neighbor.Class = ‘Galaxy’ Redshift and Color	7
Type 1D	Spectral and Photometric Data	Quasar.Class = ‘Galaxy’ and Neighbor.Class = ‘Galaxy’ Redshift and Color	1

Table 3: Count of high probability candidates (Types 1A-1D) candidates after emission line matching

The spectral comparison produced 42 final candidates, as shown in Table 3. There were 34 Type 1A candidates and 7 Type 1B candidates which remained after the emission line comparison. In addition, there was 1 Type 1D candidate remaining. The lack of type 1D candidates was due to the extended-source nature of galaxies as supposed to the point-source nature of quasars.

Statistical Analysis

A set of statistical analyses was performed on the data across different dimensions such as redshift, spatial separation and candidate groupings. The first analysis compared the spatial separation of all quasars in the candidate lists against their redshifts. The candidate quasars were binned into one of eight groups based on their redshift values ($z = 0\text{-}1, 1\text{-}2, \text{etc.}$).

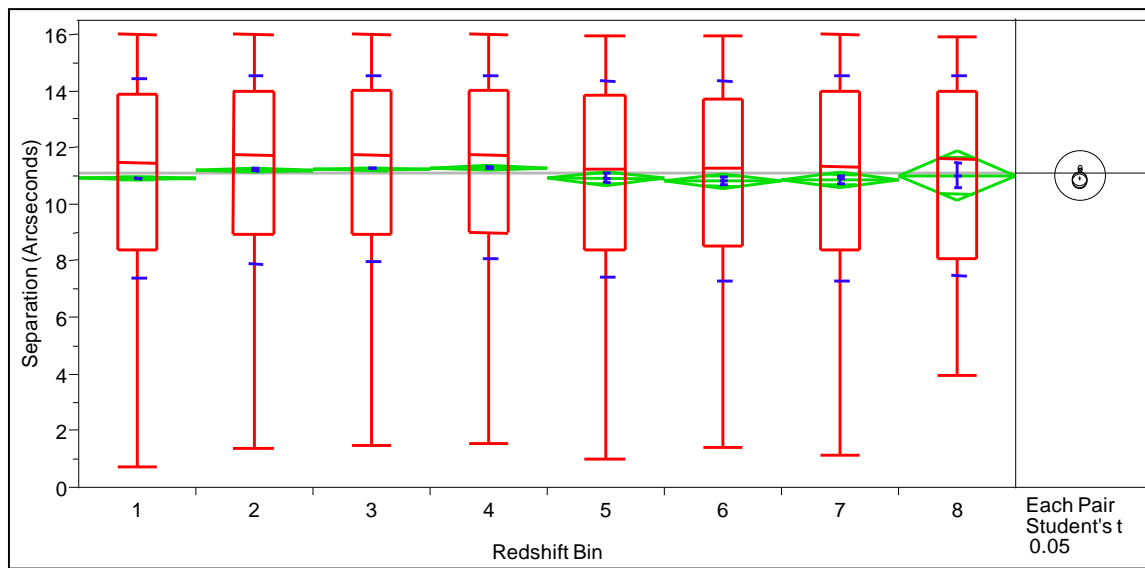


Figure 10: Analysis of spatial separation vs. redshift for all candidate quasars. A Student's t-test (comparison of means) was performed to find appropriate separation values for each redshift range.

As can be seen from Figure 10, the mean spatial separation value for all the groups lies around 11''. The differences in the mean values are not statistically significant, as the mean diamonds and Student's t-test indicate. The analysis of means confirms that the spatial separation limit is consistent across the entire redshift range.

Figure 11 shows the results from analysis of spatial separation for each group of selected candidates. The difference in means between types 1A, 1B, and 2B is not statistically significant; similarly, types 1D and 2D are quite similar. The mean difference between Type 2A and the other groups is quite significant. Type 3 is also a statistically significant group because it stands

apart from all the other groups. The results for Type 3 are consistent with the fact that Type 3 candidates are selected only using the photometric color criterion.

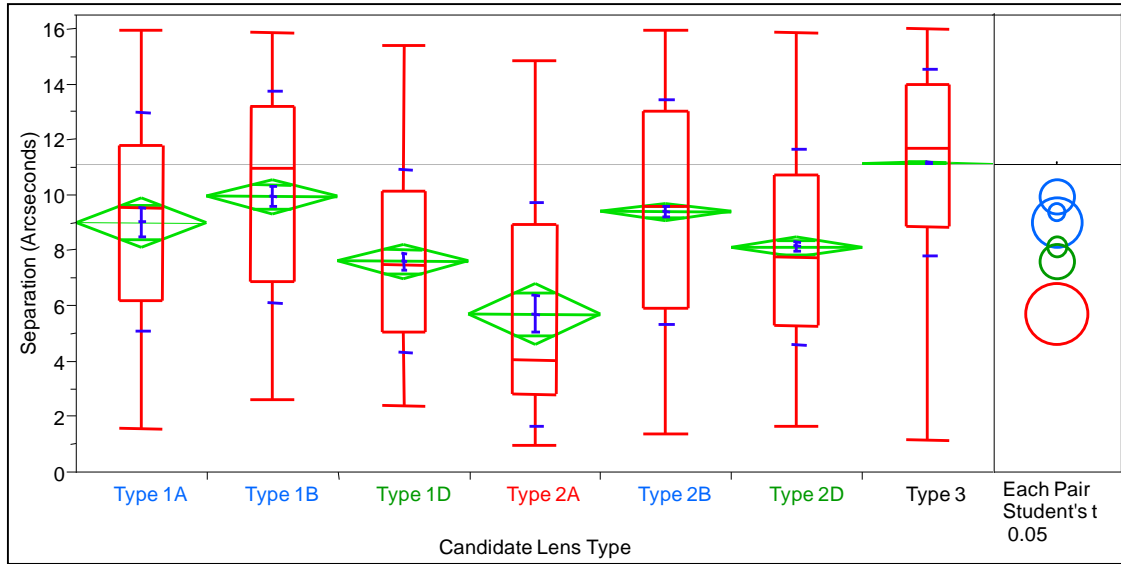


Figure 11: Analysis of spatial separation for each group of selected candidates

An outlier analysis, shown in Figure 12, was performed to determine how well the parameters of each high-probability candidate were grouped together. The analysis indicates that the redshift differences of some quasar-quasar pairs are outliers; however, the differences are still within the threshold of 0.1.

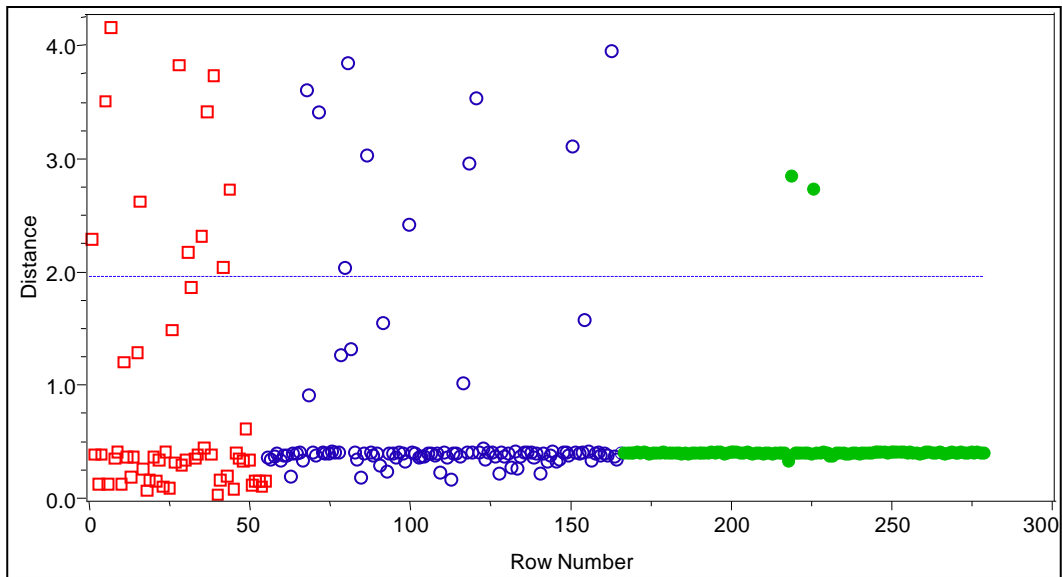


Figure 12: Outlier analysis of the redshift difference between a quasar and its neighbor. The red circles represent a pair of neighboring quasars, the green squares represent point sources, and the blue rectangles represent extended sources.

Discussion

The gravitationally lensed quasars identified by the morphological approach were compared to the control group of lensed quasars reported in the literature. The lensed quasars selected as the control group for comparison in Sivakumar (2013) were from CASTLES (CfA-Arizona Space Telescope LEns Survey), described in Kochanek et al. (1999), and the SQLS, from Inada et al. (2012). In order to use the most complete data set for comparison, the Master Lens Database, developed by Moustakas et al. (2012), was used as the control group in this research project.

However, it is not appropriate to use all of the 120 Master Lens quasar lenses as the control group. A number of lenses listed in the Master Lens Database were removed from the comparison list for a variety of reasons.

Master Lens Database Category	Number Lenses in Group
Outside SDSS Sky Coverage	24
Poor SDSS Photometry Data	38
Image Not Deblended by SDSS	24
Control Group Relevant for Comparison	34

Table 4: Percentage comparison of morphological approach results to the control group

The first group of lenses eliminated from comparison did not fall within the SDSS sky coverage.

In the Master Lens Database, there were 24 confirmed lenses outside the SDSS coverage.

Second, some of the SDSS images were of poor quality, resulting in unreliable photometric data. For example, the lensed quasar HST J01247+0352 is measured at magnitude 24. This lens system was identified using the Hubble Space Telescope. Though the object was clearly

identifiable in the Hubble image, the object was barely visible in the SDSS image due to the very low magnitude of the lensed quasar. 38 lenses fell into this category.

In order to distinguish neighboring objects from one another, the SDSS uses a process called deblending, which isolates the signals of the two objects. At separations under 2 arcseconds, the SDSS pipeline cannot differentiate between very close lenses and a single object. The 24 lensed quasars that the SDSS pipeline identified as a single object were removed from the control group. After these lenses were removed, there were 34 lensed quasars that were relevant for comparison with the results of the morphological algorithm.

The revised algorithm in this project was able to match about nine-tenths of the candidates in the control group. Table 5 and Figure 13 show the comparison between the results of this project and the control group.

Control Group Moustakas et al. (2012)	Number Lenses in Control Group	Number Matched by Morphological Algorithm	Percentage of Control Group Matched
CASTLES	14	13	93%
SQLS	16	15	94%
Other	4	2	50%
Total	34	30	88%

Table 5: Percentage comparison of morphological approach results to the control group relevant for comparison.

Since this project used data from the SDSS DR10, it had a larger set of quasars and spectra than the control group, which used earlier data sets. This approach, in addition to matching previously discovered quasar lenses, also found a number of new high-probability lensed quasar candidates not yet reported in the literature.

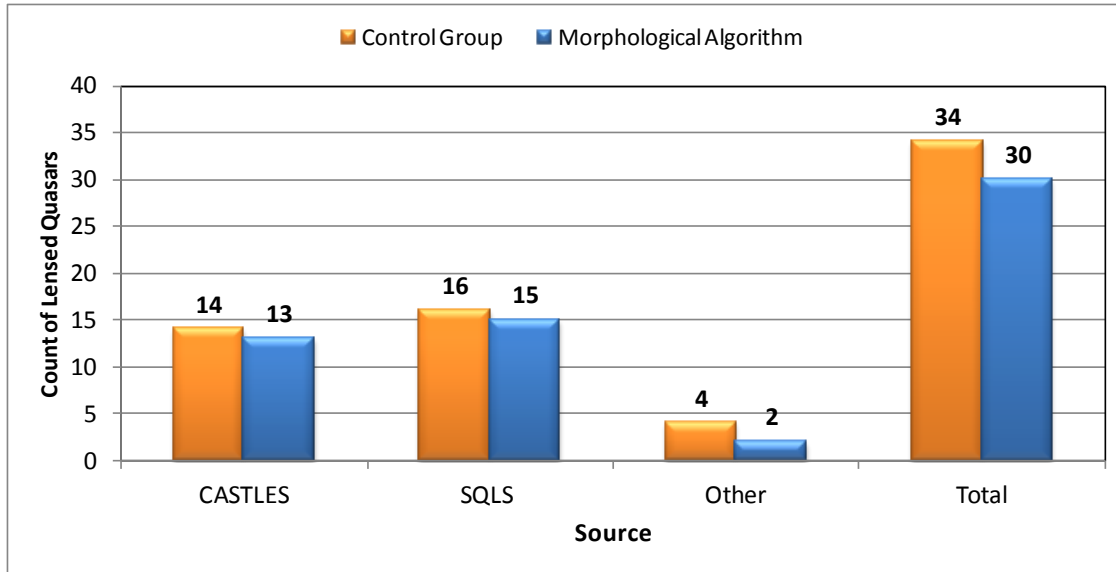


Figure 13: Comparison of morphological approach results to the control group

As previously discussed, one of the last steps of the algorithm compared the SDSS images to FIRST images. Figure 14 shows two lens candidates and their corresponding FIRST images.

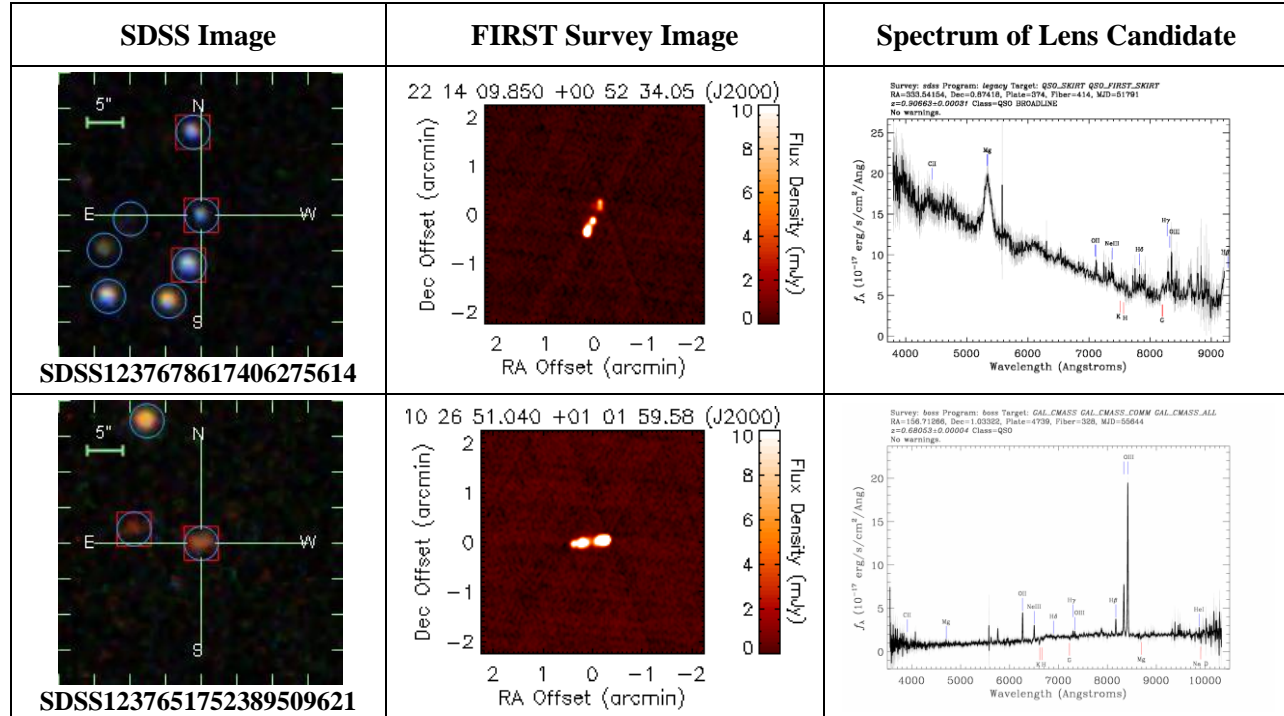


Figure 14: Examples of candidate lensed quasars matched with FIRST survey images. In each of the SDSS images, the blue circle indicates a unique object identified by the SDSS PHOTO pipeline. Objects with a red square around them possess SDSS spectra.

Figure 15 is a panel of representative lens candidates identified by the algorithm that have not been reported in the literature. A comparison of the spectrum of the target quasar with that of the lens candidate in the third column shows that the spectra have identical characteristics.

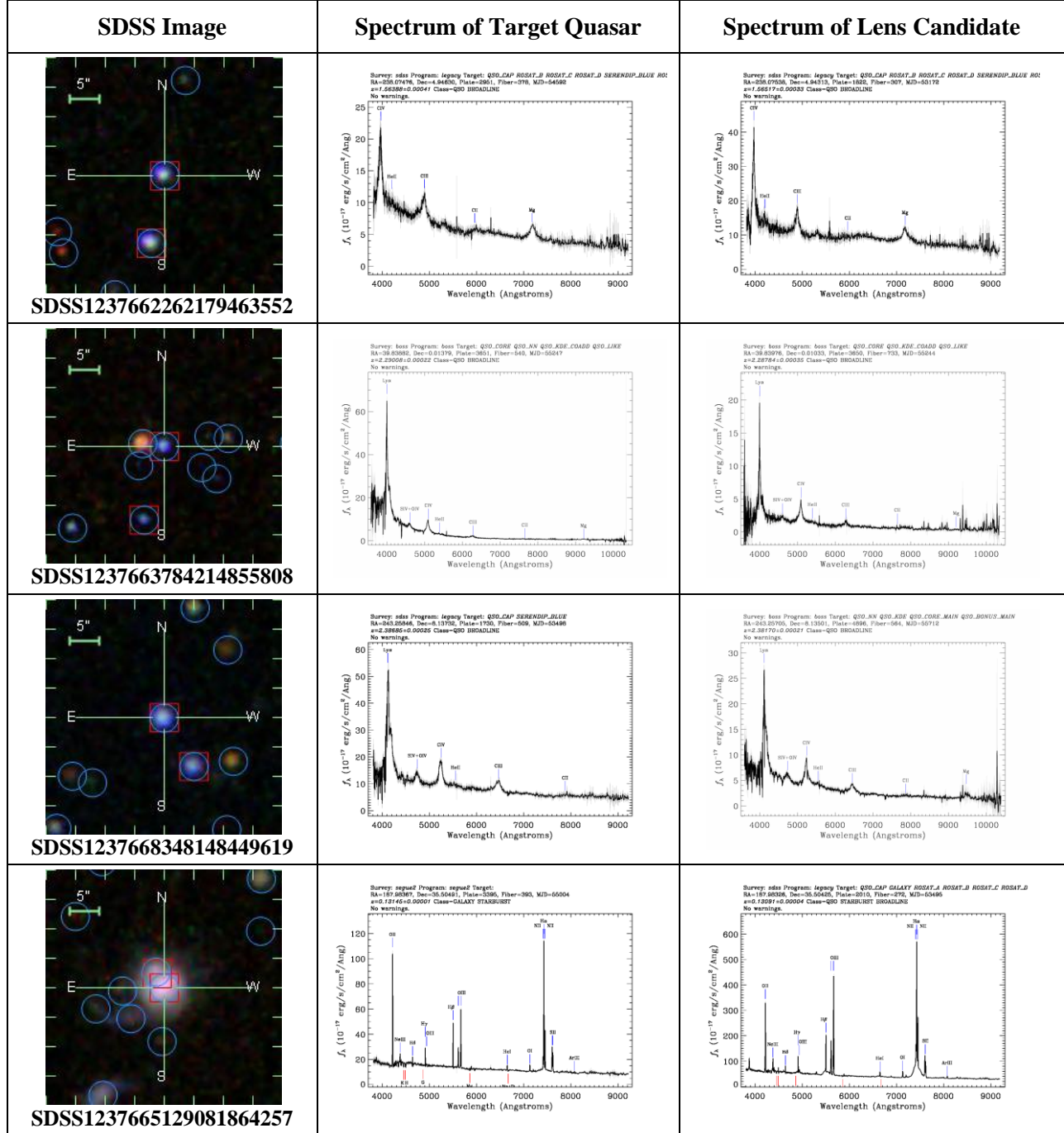


Figure 15: Examples of candidate lensed quasars identified by the algorithm

Figure 16 shows an unusual pair of lens candidate quasars that are adjacent to each other, along with what appears to be two merging galaxies. A significant amount of follow-up studies need to be completed to better understand the phenomenology of this observation.

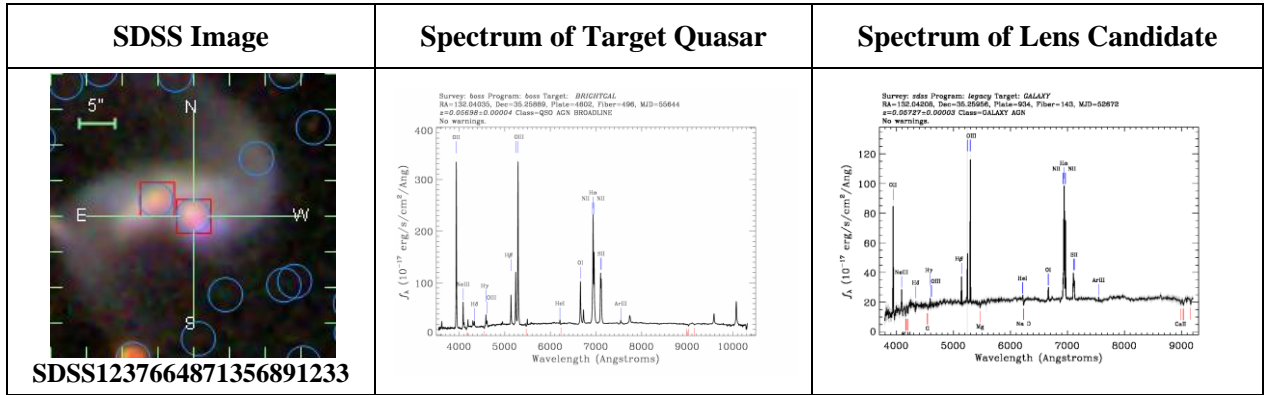


Figure 16: Unusual observation of active galactic nuclei

Conclusions

A comparison of the lensed quasar candidates identified by the present research and the lensed quasars reported in the literature leads to the conclusion that the original hypothesis of this project is well supported. In addition to matching the control group of lensed quasars, the method also found new candidates using the DR9 and DR10 data sets. The current research project, with the revised morphological algorithm and a modified data extraction strategy, overcame many shortcomings of the algorithm presented in Sivakumar (2013).

Despite the success of this approach in finding high-probability lens candidates, there are some areas where this approach could be improved. One possible source of error was that the selection criteria were too strict or loose, thus generating false negatives or positives. The classification of Type 3 candidates may also have been premature because the match was based solely on color. Errors could also have been introduced due to the procedure's dependence on the SDSS pipeline for classification of objects as QSOs, stars or galaxies. This last source of error is less likely, however, since classifications from the SDSS pipeline are generally reliable.

Based on the research work performed in this project, it can be concluded that the morphological approach is effective in identifying lensed quasar candidates. Follow-up observations of these candidates using large telescopes are necessary to confirm the lensing effects. These detailed observations will also eliminate binary quasars, which can easily be mistaken for lensed quasars based solely on SDSS data.

A future extension of this project currently under consideration is to use PSF (point spread function)-based criteria to deblend blended lens images identified by the SDSS PHOTO pipeline.

This extension will almost double the number of lensed quasars that can be identified by the morphological algorithm.

Further research to improve the accuracy of the algorithm is being pursued in follow-up projects. In particular, the accuracy could be improved using a complete set of spectral data, more detailed statistical analyses to refine the threshold value, and an implementation of additional validation steps in the algorithm. Opportunities to apply the results of this work to constrain cosmological parameters through lensing statistics (distribution of redshifts and separations) are also being explored.

Reference List

1. Ahn, C. P., Alexandroff, R., Allende P. C., Anderson, S. F., Anderton, T., Andrews, B. H., et al. (2012). The Ninth Data Release of the Sloan Digital Sky Survey: First Spectroscopic Data from the SDSS-III Baryon Oscillation Spectroscopic Survey. *The Astrophysical Journal Supplement*, 203, 21.
2. Ahn, C. P., Alexandroff, R., Allende P. C., Anders, F., Anderson, S. F., Anderton, T., et al. (2013). The Tenth Data Release of the Sloan Digital Sky Survey: First Spectroscopic Data from the SDSS-III Apache Point Observatory Galactic Evolution Experiment. *The Astrophysical Journal Supplement*, submitted.
3. Becker, R. H., White, R. L., & Helfand, D. J. (1995). The FIRST Survey: Faint Images of the Radio Sky at Twenty Centimeters. *The Astrophysical Journal Supplement*, 450, 559.
4. Browne, I. W. A., Wilkinson, P. N., Jackson, N. J. F., Myers, S. T., Fassnacht, C. D., Koopmans, L. V. E., et al. (2003). The Cosmic Lens All-Sky Survey - II. Gravitational lens candidate selection and follow-up. *Monthly Notice of the Royal Astronomical Society*, 341, 13-32.
5. Inada, N., Oguri, M., Becker, R.H., Shin, M., Richards, G.T., Hennawi, J. F., White, R. L., et al. (2008). The Sloan Digital Sky Survey Quasar Lens Search. II. Statistical Lens Sample from the Third Data Release. *The Astronomical Journal*, 135, 496-511.
6. Inada, N., Oguri, M, Shin, M., Kayo, I., Strauss, M.A., Morokuma, T., et al. (2012). The Sloan Digital Sky Survey Quasar Lens Search. V. Final Catalog from the Seventh Data Release. *The Astronomical Journal*, 143, 119.
7. Kochanek, C. S., Falco, E. E., Impey, C. D., Lehár, J., McLeod, B. A., Rix, H.W., (1999). Results from the CASTLES survey of gravitational lenses. *AIP Conference Proceedings*, 470, 163-175.
8. Moustakas, L. A., Brownstein, J. R., Fadely, R., Fassnacht, C. D., Gavazzi, R., Goodsall, T., et al. (2012). The Orphan Lenses Project. *American Astronomical Society, AAS Meeting*, #219, #146.01.
9. Maoz, D., Bahcall, J. N., Schneider, D. P., Bahcall, N. A., Djorgovski, S., Doxsey, R., et al. (1993). The Hubble Space Telescope Snapshot Survey. IV - A summary of the search for gravitationally lensed quasars. *The Astrophysical Journal*, 409, 28-41.

10. The Master Lens Database [Computer Database]. Salt Lake City, UT: The University of Utah.
11. Oguri, M., Inada, N., Pindor, B., Strauss, M.A., Richards, G.T., Hennawi, J. F., Turner, E. L., et al. (2006). The Sloan Digital Sky Survey Quasar Lens Search. I. Candidate Selection Algorithm. *The Astronomical Journal*, 132, 999-1013.
12. Oguri, M., Inada, N., Strauss, M.A., Kochanek, C.S., Kayo, I., Shin, M., et al. (2012). The Sloan Digital Sky Survey Quasar Lens Search. VI. Constraints on Dark Energy and the Evolution of Massive Galaxies. *The Astronomical Journal*, 143, 120-134.
13. Richards, G. T., Fan, X., Schneider, D. P., Vanden Berk, D. E., Strauss, M. A., York, D. G., et al. (2001). Colors of 2625 Quasars at $0 < z < 5$ Measured in the Sloan Digital Sky Survey Photometric System. *The Astronomical Journal*, 121, 2308-2330.
14. Schechter, P. L., Gregg, M. D., Becker, R. H., Helfand, D. J., & White, R. L. (1998). The First FIRST Gravitationally Lensed Quasar: FBQ 0951+2635. *The Astronomical Journal*, 115, 1371-1376.
15. SDSS Query/CasJobs [Computer program]. Cambridge, MA: Harvard University.
16. Sivakumar, P. (2013). Identification of Gravitationally Lensed Quasars: A Morphological Approach. *Illinois Junior Academy of Science, IJAS State Conference*.
17. Turner, E.L., Ostriker, J. P., Gott III J. R. (1984). The statistics of gravitational lenses: the distributions of image angular separations and lens redshifts. *The Astrophysical Journal*, 284, 1-22.
18. Wright E. L. (2006). A Cosmology Calculator for the World Wide Web. *The Publications of the Astronomical Society of the Pacific*, 118, 1-22.

Acknowledgments

I wish to thank Dr. Brian Nord at the Center for Particle Astrophysics at the Fermi National Accelerator Laboratory (FNAL) for giving me a deep understanding of the SDSS camera operation and data pipeline. I would also like to acknowledge Dr. Chris Stoughton, also of the Center for Particle Astrophysics at FNAL, for introducing me to the power of the Python and SciPy programming environments. Many thanks to my father for teaching me effective ways to use SQL to extract and manipulate data from the SDSS Science Archive Server. Finally, I wish to thank the faculty of the Saturday Morning Physics program at Fermilab for inspiring me to pursue research in the field of astrophysics and cosmology.

Official SDSS-III Acknowledgement Statement: Funding for SDSS-III has been provided by the Alfred P. Sloan Foundation, the Participating Institutions, the National Science Foundation, and the U.S. Department of Energy Office of Science. The SDSS-III web site is <http://www.sdss3.org/>. SDSS-III is managed by the Astrophysical Research Consortium for the Participating Institutions of the SDSS-III Collaboration including the University of Arizona, the Brazilian Participation Group, Brookhaven National Laboratory, University of Cambridge, Carnegie Mellon University, University of Florida, the French Participation Group, the German Participation Group, Harvard University, the Instituto de Astrofisica de Canarias, the Michigan State/Notre Dame/JINA Participation Group, Johns Hopkins University, Lawrence Berkeley National Laboratory, Max Planck Institute for Astrophysics, Max Planck Institute for Extraterrestrial Physics, New Mexico State University, New York University, Ohio State University, Pennsylvania State University, University of Portsmouth, Princeton University, the Spanish Participation Group, University of Tokyo, University of Utah, Vanderbilt University, University of Virginia, University of Washington, and Yale University